View metadata, citation and similar papers at core.ac.uk
brought to you by CORE
provided by AIR Universita degli studi di Milano

ANTIOXIDANTS & REDOX SIGNALING
Volume 25, Number 11, 2016
© Mary Ann Liebert, Inc.
DOI: 10.1089/ars.2015.6582

ORIGINAL RESEARCH COMMUNICATION

A Peculiar Formula of Essential Amino Acids Prevents Rosuvastatin Myopathy in Mice

Giuseppe D'Antona,[1,*] Laura Tedesco,[2,*] Chiara Ruocco,[2,*] Giovanni Corsetti,[3] Maurizio Ragni,[2] Andrea Fossati,[2] Elisa Saba,[4] Francesca Fenaroli,[4] Mery Montinaro,[4] Michele O. Carruba,[2] Alessandra Valerio,[4] and Enzo Nisoli[2]

Abstract

Aims: Myopathy, characterized by mitochondrial oxidative stress, occurs in ~10% of statin-treated patients, and a major risk exists with potent statins such as rosuvastatin (Rvs). We sought to determine whether a peculiar branched-chain amino acid-enriched mixture (BCAAem), found to improve mitochondrial function and reduce oxidative stress in muscle of middle-aged mice, was able to prevent Rvs myopathy. ***Results:*** Dietary supplementation of BCAAem was able to prevent the structural and functional alterations of muscle induced by Rvs in young mice. Rvs-increased plasma 3-methylhistidine (a marker of muscular protein degradation) was prevented by BCAAem. This was obtained without changes of Rvs ability to reduce cholesterol and triglyceride levels in blood. Rather, BCAAem promotes *de novo* protein synthesis and reduces proteolysis in cultured myotubes. Morphological alterations of C2C12 cells induced by statin were counteracted by amino acids, as were the Rvs-increased atrogin-1 mRNA and protein levels. Moreover, BCAAem maintained mitochondrial mass and density and citrate synthase activity in skeletal muscle of Rvs-treated mice beside oxygen consumption and ATP levels in C2C12 cells exposed to statin. Notably, BCAAem assisted Rvs to reduce oxidative stress and to increase the anti-reactive oxygen species (ROS) defense system in skeletal muscle. ***Innovation and Conclusions:*** The complex interplay between proteostasis and antioxidant properties may underlie the mechanism by which a specific amino acid formula preserves mitochondrial efficiency and muscle health in Rvs-treated mice. Strategies aimed at promoting protein balance and controlling mitochondrial ROS level may be used as therapeutics for the treatment of muscular diseases involving mitochondrial dysfunction, such as statin myopathy. *Antioxid. Redox Signal.* 25, 595–608.

Introduction

STATINS (3-HYDROXY-3-METHYLGLUTARYL-COENZYME A [HMG-CoA] reductase inhibitors) are currently the most widely prescribed lipid-lowering drugs, and their use is expected to continue to grow alongside the increasing elderly population and the diffusion of new guidelines on the treatment of blood cholesterol (2013) of the American College of Cardiology and American Heart Association (46).

Despite being relatively safe drugs, all statins are associated with a significantly elevated risk of myopathy, which can range in severity from asymptomatic increases in creatine kinase (CK) and muscle weakness, aches, and fatigue to fatal rhabdomyolysis. While the incidence of rhabdomyolysis is fortunately very low (0.1% of all statin users), the number of patients who do not tolerate statins due to myopathy-like symptoms is significant (1–10%) (12, 21, 44, 60). Although this represents a relatively small risk and almost certainly does not outweigh the benefits in cardiovascular risk modification, the vast number of patients prescribed or to be prescribed statin medication results in a large absolute number of myopathic complications. Rosuvastatin (Rvs), the most prescribed brand name in the United States, has a significantly higher risk of an abnormally raised CK than other statins, including simvastatin, pravastatin, or atorvastatin (64).

[1]Department of Public Health, Experimental and Forensic Medicine, Pavia University, Pavia, Italy.
[2]Department of Medical Biotechnology and Translational Medicine, Center for Study and Research on Obesity, Milan University, Milan, Italy.
Departments of [3]Clinical and Experimental Sciences and [4]Molecular and Translational Medicine, Brescia University, Brescia, Italy.
*These authors contributed equally to this work.

Innovation

Statin use in dyslipidemia is often hampered by unacceptable side effects at the expense of skeletal muscle. In the current study, we demonstrate that an amino acid formula enriched in BCAAs is able to prevent muscular damage induced by Rvs through induction of *de novo* protein synthesis and decrease of protein breakdown. We have also shown here that amino acids preserve mitochondrial efficiency and ameliorate the control of oxidative stress in the statin-treated mice and muscle cells. Tailored amino acid formulas may be exploited as potential therapeutics to preserve protein and mitochondrial homeostasis in diseases such as statin myopathy.

Very intensive efforts, including the high-throughput analysis, have been made; nevertheless, the mechanisms involved in statin-induced myopathy are poorly understood (35). Although statin-mediated lowering of cholesterol and ubiquinone (coenzyme Q) or mitochondrial dysfunctions have been widely investigated, no really efficacious aid for statin toxicity was found so far (20, 22). These effects of statins would predispose the myocytes to membrane alterations, increased reactive oxygen species (ROS) production, and apoptosis (10, 11, 21). Importantly, supplementation with coenzyme Q or antioxidants, such as selenium and vitamin E, or other products targeting either cell respiration or oxidative stress has been found scarcely effective (7, 8, 55).

Statins inhibit the mechanistic target of rapamycin (mTOR) pathway that regulates protein synthesis and cell growth in vascular smooth muscle (65, 66) and cancer cells (25, 70). Accordingly, statins repress protein synthesis in C2C12 myocytes (59) and increase proteolysis through the atrogin system in skeletal muscles of mouse and zebrafish (13, 30). In this study, we investigated the efficacy of a peculiar formula of essential amino acids enriched in BCAAs to prevent myopathy in mice treated with Rvs. The branched-chain amino acid-enriched mixture (BCAAem) was previously found to improve sarcopenia in elderly people, promote mitochondrial biogenesis, and reduce ROS in cultured myocytes and skeletal muscles of middle-aged mice, through endothelial nitric oxide synthase and mTOR pathways (16, 63). The present results demonstrate that BCAAem supplementation prevents the Rvs-induced structural and functional deteriorations of skeletal muscles in adult mice, without affecting the cholesterol-lowering capability of the statin. These healthy effects are accompanied by rescue of *de novo* protein synthesis and decrease of proteolysis and mitochondrial dysfunction, with less oxidative stress. This suggests that dietary supplementation of selective amino acid mixtures may be a promising strategy to prevent statin myopathy in humans.

Results

BCAAem does not impair the cholesterol-lowering capacity of Rvs

Dietary supplementation with BCAAem was found to change selectively the levels of free amino acids in plasma, to increase mitochondrial biogenesis, and to improve muscle functions in sedentary and exercised middle-aged, but not young, mice (15, 16). First, in the present work, we verified if BCAAem supplementation influenced the ability of Rvs to lower plasma lipid levels. Total cholesterol (T-Cho) and triglycerides (TGs) were measured in 8-week-old male apolipoprotein E gene-deficient (ApoE-KO) mice fed with a high-fat diet (HFD) for 12 weeks (*i.e.*, hyperlipidemic mice), and then treated with Rvs, BCAAem, and Rvs plus BCAAem for 1 month. Before HFD exposure, the T-Cho levels were 11.6 ± 0.5 m*M* and increased with time up to 50 ± 2.5 m*M*. When compared with untreated mice, Rvs reduced T-Cho and TGs by about $35\% \pm 5\%$ and $41\% \pm 6\%$ (Fig. 1), as previously described (29, 37, 51). Notably, BCAAem, ineffective when administered alone, left unchanged the Rvs ability to lower T-Cho and rather potentiated the effect of statin on TG levels (Fig. 1). While not affecting daily food intake, Rvs treatment significantly reduced mice body weight (BW) (27.3 ± 0.8 g in Rvs-treated *vs.* 30.9 ± 1.2 g in untreated mice; $p < 0.05$). BCAAem did not affect BW either when administered alone or in combination with Rvs (data not shown).

BCAAem prevents Rvs myopathy

Next, young (2-month-old) C57BL/6JN mice (*i.e.*, normolipidemic mice) were used, and Rvs (20 mg/kg/day) and BCAAem (1.5 mg/g BW/day) were administered alone or in combination for 1 month. BW, food intake, and water consumption were unchanged after treatments with Rvs, BCAAem, or Rvs plus BCAAem (Supplementary Table S1; Supplementary Data are available online at www.liebertpub.com/ars). Serum CK levels, a proxy for muscle damage widely used as a biomarker of statin-induced myopathy (57), were threefold higher in Rvs-treated than untreated mice (Fig. 2A). BCAAem, unable to modify the enzyme levels when administered alone, markedly blunted the statin-increased CK (Fig. 2A). Gross histology analysis by hematoxylin–eosin (HE) staining did not show major changes of fiber architecture and clear signs of cellular degenerative processes (*i.e.*, calcification, fibrosis, and necrosis) in gastrocnemius of treated mice (Fig. 2B). Consistently, toluidine blue staining highlights numerous irregular nuclei, with condensed chromatin, in gastrocnemius muscle of Rvs-treated animals differently from mice exposed to statin and amino acid combination or untreated

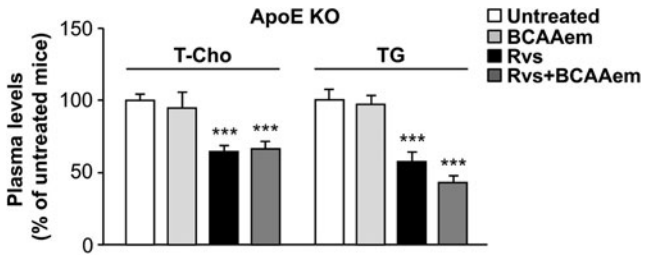

FIG. 1. BCAAem supplementation does not interfere with the plasma lipid-lowering capacity of Rvs in hyperlipidemic mice. Plasma T-Cho and TG of ApoE-KO mice ($n = 10$/group) fed with HFD for 12 weeks and then treated with Rvs and BCAAem alone or in combination for 4 weeks. Data are reported as percentage expression over the untreated mice. ***$p < 0.001$ *versus* untreated mice. Data are represented as mean ± SEM. ApoE-KO, apolipoprotein E gene-deficient; BCAAem, branched-chain amino acid-enriched mixture; HFD, high-fat diet; Rvs, rosuvastatin; SEM, standard error of the mean; T-Cho, total cholesterol; TG, triglyceride.

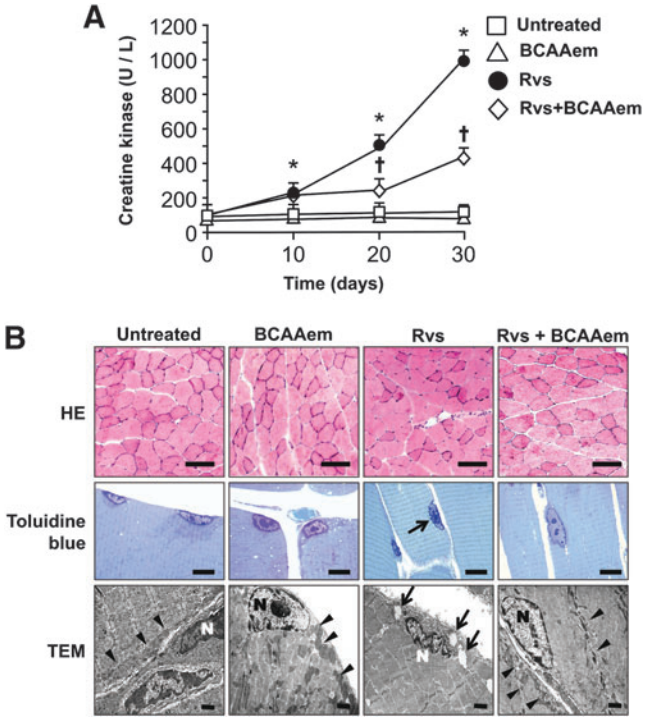

FIG. 2. BCAAem supplementation protects muscle from damage induced by Rvs. (A) Serum CK level measures in mice ($n = 20$/group) treated for 1 month with Rvs and BCAAem alone or in combination. The time course of CK levels was evaluated at time 0 and after 10, 20, and 30 days of treatment. The enzyme activity is expressed in U/L as mean ± SEM. $^{*}p < 0.05$ *versus* untreated group; $^{\dagger}p < 0.05$ *versus* Rvs group. **(B)** HE staining did not show major changes of fiber architecture and clear signs of cellular degenerative processes in gastrocnemius muscle. Scale bar, 100 μm. Toluidine blue staining showed that although the organization of sarcomeres appeared regular, nuclei appeared strongly wavy shaped (*arrow*), with condensed chromatine on the inner surface of nuclear envelope and inside the nuclear matrix. BCAAem supplementation prevented these nuclear alterations. Scale bar, 10 μm. TEM analysis showed that Rvs treatment did cause irregular nuclei with condensed chromatin near the inner nuclear membrane. The perinuclear cytoplasm had wide empty spaces (*arrows*), scarce and small mitochondria with dilated cristae, and little electron-dense matrix. Rvs plus BCAAem treatment prevented these morphological damages and preserved nuclear morphology, although mitochondria (*arrowheads*) tended to be smaller compared with untreated and BCAAem-treated mice. N, nucleus. Scale bar: 1 nm. Analyses were performed in two animals per group. Representative stained images from at least three independent experiments are reported. All experiments were conducted in C57BL/6JN mice. CK, creatine kinase; HE, hematoxylin–eosin. To see this illustration in color, the reader is referred to the web version of this article at www.liebertonline.com/ars

ones (Fig. 2B). These morphological aspects were further investigated by transmission electron microscopy. The ultrastructural integrity of skeletal muscle fibers was compromised in Rvs, unlike Rvs plus BCAAem-treated animals; muscle damage was restricted to the intracellular space of individual fibers, predominantly affecting (swelling) the triad structure (formed by T-tubule and sarcoplasmic reticulum cisternae) typically located at the junction between A and I bands of sarcomere, and the subsarcolemmal myofibrillar system (Fig. 2B). Disorganized mitochondria and shrunken nuclei were evident in Rvs-treated animals, but not in Rvs-treated mice supplemented with BCAAem. We evaluated the effects on Rvs-myopathy, measured as CK levels, toluidine blue staining, and electron microscopy of different doses of BCAAem besides 1.5 mg/g BW/day (*i.e.*, 0.15, 0.75, and 3.0 mg/g BW/day). No statistically significant effect was observed at the lower doses, while 3.0 mg/g BW/day was not superior to 1.5 mg/g/day, as opposed to statin damage (data not shown). Thus, we subsequently used the last dose of BCAAem in all of the experiments carried out in C57BL/6JN mice.

BCAAem preserves muscle function in Rvs-treated mice

It is well known that statins cause a loss of skeletal muscle mass paralleled by mitochondrial impairment (68). Although muscle weight (MW) and MW relative to the BW were not changed by Rvs (Supplementary Fig. S1A, B), we observed that the fiber cross-sectional areas (CSAs) of vastus lateralis and gastrocnemius muscle were reduced significantly in Rvs-treated mice and these changes were prevented by BCAAem supplementation (Fig. 3A). The MW and MW/BW ratio and the CSA values were not changed by BCAAem supplementation *per se* (Fig. 3A and data not shown).

Next, to assess muscle function, we investigated whole endurance capacity *in vivo* by means of horizontal and uphill treadmill tests. Notably, starting at 10 days of treatment, Rvs mice showed significantly lower time to exhaustion in both treadmill tests compared with untreated animals (Fig. 3B, C). On the contrary, the Rvs plus BCAAem mice showed higher endurance capacity than Rvs mice at all time points, and their performance was comparable with that of untreated at 20 and 30 days of treatment (Fig. 3B, C). No functional changes were observed after BCAAem supplementation *per se* (Fig. 3B, C).

To confirm whether the observed changes of *in vivo* performance were mirrored by *ex vivo* changes in skeletal muscle preparations, we measured both the absolute and normalized tetanic forces and the rates of fatigue development in intact tibialis muscle. The muscle absolute and normalized tensions were lower in Rvs than Rvs plus BCAAem combination (Fig. 3D, E). Moreover, Rvs induced a higher susceptibility to fatigue than Rsv plus BCAAem or untreated (Fig. 3F). Interestingly, Rvs and Rvs plus BCAAem did not show any functional effect on soleus muscle (data not shown).

BCAAem promotes de novo *protein synthesis and reduces proteolysis in cultured myotubes*

Next, we sought to investigate the underlying mechanism(s) of BCAAem effect on statin myopathy. Cultured C2C12-derived myocytes were exposed to increasing Rvs concentrations. Differently from vehicle treatment, 24 h of Rvs treatment caused myocyte thinning and damage (Fig. 4A and data not shown). This effect was detectable in a range of Rvs concentrations superimposable to that observed in plasma of Rvs-treated patients. Almost complete myocyte loss was observed after 5 days of 50 μM Rvs treatment (data not shown). Importantly, yet unable to change myotube

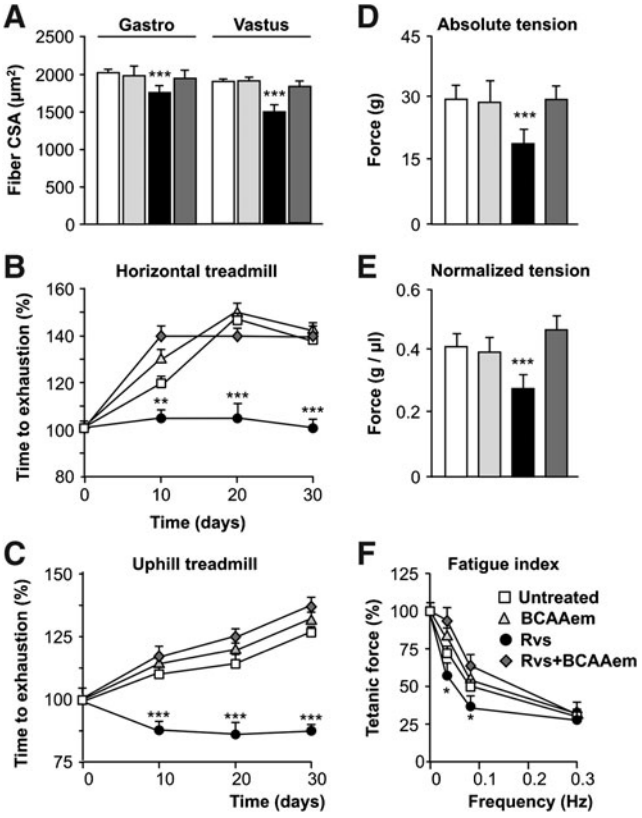

FIG. 3. BCAAem supplementation restores skeletal muscle function and structure in Rvs-treated mice. (A) Fiber CSA of gastrocnemius and vastus lateralis muscle. **(B)** and **(C)** Initial time to reach the exhaustion following horizontal and uphill treadmill tests as expression of endurance capacity of mice at time 0 and after 10, 20, and 30 days of treatments. **(D)** and **(E)** Absolute (g) and normalized tetanic forces over muscle volume expressed in microliters (g/μl) were evoked by 110 Hz for 500 ms. **(F)** Fatigue index in intact tibialis muscle, measured as the tetanic force drop after different stimulation frequencies (from 0.03 to 0.9 Hz, 500 ms) compared with the maximal tetanic force and expressed as % over untreated mice. All data were obtained from C57BL/6JN mice treated with Rvs and BCAAem alone or in combination for 1 month ($n = 20$/group). $^{**}p < 0.01$, $^{***}p < 0.001$ *versus* corresponding untreated mice. Data represent mean ± SEM. CSA, cross-sectional area.

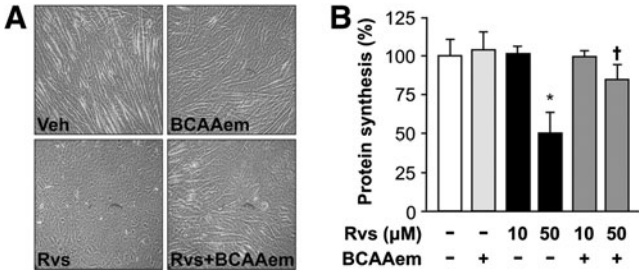

FIG. 4. BCAAem supplementation antagonized the damage induced by Rvs through the modulation of *de novo* protein synthesis in C2C12 myotubes. (A) Morphological changes of C2C12 myotubes after 24 h of treatment with Veh or Rvs (50 μM) with or without BCAAem (the images are representative of five separate experiments). **(B)** *De novo* protein synthesis was expressed as percentage over vehicle-treated cells exposed. C2C12 myotubes were exposed to Rvs (10 or 50 μM) and BCAAem (1×) alone or in combination for 24 h ($n = 5$ experiments).$^{*}p < 0.05$ *versus* vehicle-treated cells; $^{\dagger}p < 0.05$ *versus* Rvs-treated cells. All data represent mean ± SEM. Veh, Vehicle.

morphology when added alone, BCAAem robustly antagonized the morphological effects of statin (Fig. 4A).

Since it is known that amino acids are able to modulate protein synthesis and degradation in muscle (41), we investigated whether BCAAem was able to counteract the effect of Rvs on these processes. According to Tuckow *et al.* (59), treatment of C2C12 myotube cultures with Rvs for 24 h resulted in significant reduction of *de novo* protein synthesis, which was prevented by BCAAem (Fig. 4B). BCAAem alone left unchanged *de novo* protein synthesis compared with vehicle-treated cells (Fig. 4B).

Plasma 3-methylhistidine (3-MeH) is considered a marker of protein degradation in skeletal muscle (28). We measured the circulating 3-MeH levels in mice, and we found that BCAAem counteracted the Rvs-increased proteolysis (Supplementary Fig. S2). Next, we measured rates of protein breakdown in Rvs-treated myotubes. Similarly to what was observed with lovastatin treatment (30), we found that Rvs treatment time- and concentration-dependently increased *atrogin-1* mRNA levels in C2C12 myocytes (Fig. 5A). Particularly, myocyte exposure to 50 μM Rvs significantly induced *atrogin-1* expression after 6 h and caused a threefold induction after 48 h (Fig. 5B). As shown in Figure 5C, also *atrogin-1* protein levels were increased 2.5-fold after 48 h of Rvs exposure. BCAAem, which had no effects when added alone, counteracted the *atrogin-1* mRNA and protein levels increased by Rvs (Fig. 5B, C). Together, these experiments suggest that the amino acid mixture counterbalanced Rvs-induced muscle injury through the modulation of *de novo* protein synthesis and breakdown.

Rvs and BCAAem modulate BCAA metabolism

Protein turnover is linked to catabolism of BCAAs (*i.e.*, leucine, isoleucine, and valine) (34) and the most active system for the oxidation of BCAAs is located in skeletal muscle (52). Thus, we investigated the expression and activity of mitochondrial branched-chain aminotransferase (BCATm) and branched-chain α-keto acid dehydrogenase (BCKDH), the first two enzymes of BCAA degradation. Increased expression of BCKDH, but not of BCATm, was observed in vastus lateralis muscle after treatment with Rvs, alone or in combination with BCAAem (Fig. 6A and Supplementary Fig. S3A). Accordingly, a robust increase of BCKDH activity, unlike BCATm, was observed in C2C12 cells exposed to 50 μM Rvs (Fig. 6B and Supplementary Fig. S3B). A concomitant treatment with BCAAem further activated the enzyme (Fig. 6B). Predictably, amino acids were effective *per se* when added alone on BCKDH, unlike BCATm, levels and activity (Fig. 6A, B and Supplementary Fig. S3A, B). As the BCKDH activity is attenuated by BCKDH kinase (BCKDK) that phosphorylates the enzyme (52), we assessed the expression of BCKDK. No changes of the BCKDK mRNA levels in vastus lateralis muscle were induced by treatments with Rvs, amino acids, or their combination in muscle (Fig. 6C) and C2C12 cells (data not

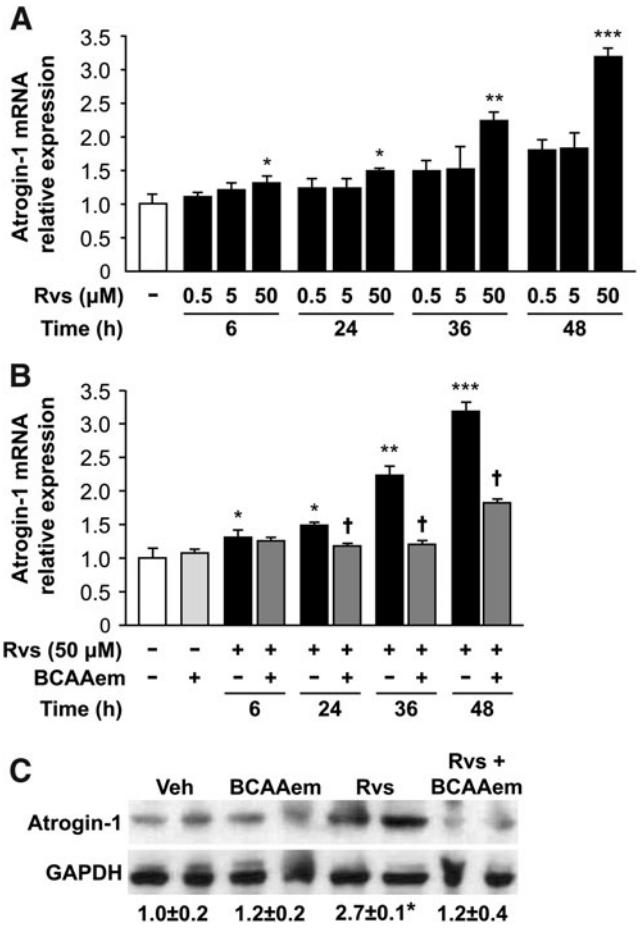

FIG. 5. BCAAem supplementation normalized *atrogin-1* gene expression in Rvs-treated myotubes. *Atrogin-1* mRNA was analyzed by means of quantitative RT-PCR. GAPDH was served as the standard. **(A)** Dose and time course analysis of *atrogin-1* mRNA levels. **(B)** C2C12 myotubes were treated with 50 μM Rvs for 6, 24, 36, and 48 h, with or without BCAAem (1×) for 24 h. Relative expression value of the vehicle-treated cells was taken as 1.0 ($n = 5$ experiments). **(C)** Atrogin-1 protein levels detected by immunoblot in C2C12 myotubes treated with 50 μM Rvs and BCAAem (1×) for 48 h. One experiment representative of three reproducible ones was shown, with relative values of densitometric analysis referred to the vehicle-treated cells taken as 1.0. GAPDH was the loading control. $^{*}p < 0.05$, $^{**}p < 0.01$ *versus* vehicle-treated cells; $^{\dagger}p < 0.05$ *versus* Rvs-treated cells. All data are expressed as mean ± SEM. GAPDH, glyceraldehyde-3-phosphate dehydrogenase; RT-PCR, reverse transcriptase–polymerase chain reaction.

shown). Thus, the increased BCKDH activity observed with Rvs and Rvs plus BCAAem seems to be linked to its increased expression.

BCAAem prevents mitochondrial defects

Given the role of mitochondria dysfunction in the statin-induced myopathy development (32, 53) and the ability of BCAAem to boost mitochondrial activity (16), we asked whether amino acid supplementation could rescue Rvs myopathy by acting on mitochondria. Thus, citrate synthase (CS) activity was measured both in skeletal muscles and C2C12 myocytes. The CS activity was found robustly decreased in gastrocnemius and tibialis muscles of Rvs-treated mice compared with untreated ones (Fig. 7A). BCAAem fully restored the enzyme activity in Rvs mice without changing it in the Rvs-untreated mice (Fig. 7A). To confirm further that the effects of BCAAem were due to increased oxidative, but not glycolytic, metabolism, we measured lactate dehydrogenase activity. No marked changes were found in the Rvs and Rvs plus BCAAem-treated mice compared with untreated mice in all muscles studied (data not shown), confirming that oxidative metabolism is the major biochemical target of amino acids (17). Accordingly, the mitochondrial mass and density, which were markedly reduced in gastrocnemius of the Rvs-treated mice, were restored to values of untreated mice by BCAAem (Fig. 7B, C). BCAAem was unable to affect mitochondrial mass and density in skeletal muscle of Rvs-untreated mice.

The observed *in vivo* effects on mitochondria were confirmed *in vitro* in C2C12 myocytes. Notably, BCAAem was able to improve mitochondrial function by increasing mitochondrial respiration and oxidative phosphorylation (Fig. 7D, E) and restoring full ATP production (Fig. 7F). Collectively, these findings support the idea that Rvs-induced myopathy would derive from defective oxidative metabolism and that the BCAAem supplementation would oppose to it acting on mitochondrial efficiency.

BCAAem assists Rvs to reduce oxidative stress

As one consequence of mitochondrial dysfunction and cause of oxidative damage is the accumulation of ROS (61), we studied different ROS markers in vastus lateralis muscle after Rvs and BCAAem treatment. When compared with untreated animals, mitochondrial H_2O_2 release was increased, while basal/total aconitase activity ratio was decreased by Rvs (Fig. 8A, B). These differences were less pronounced following contemporary supplementation of BCAAem (Fig. 8A, B). On the other hand, Rvs reduced lipid peroxidation in vastus lateralis muscle, and BCAAem strengthened this reduction (Fig. 8C). Accordingly, the amount of 8-hydroxy-2′-deoxyguanosine (8-OHdG), a marker of oxidative DNA damage, was reduced in both mitochondrial and nuclear DNA from vastus lateralis of Rvs-treated mice; this effect was boosted by BCAAem, which was ineffective when administered alone (Fig. 8D).

Moreover, also the alternative ROS-producing system NADPH oxidase was found to play some, yet limited, role. In fact, $p47^{phox}$ (cytosolic NADPH oxidase) (26) mRNA was decreased by BCAAem in vastus lateralis muscle of Rvs-treated mice, even if $gp91^{phox}$ and Rac1 (membrane NADPH oxidase) mRNA levels were unchanged, as confirmed by protein level analysis (Supplementary Fig. S4A, B).

Because oxidative stress ignites the anti-ROS defense system, we investigated the expression of anti-ROS enzymes in gastrocnemius of statin- and/or amino acid-treated mice. Superoxide dismutase 1 and 2 (SOD1 and SOD2) and catalase mRNAs and proteins were increased by Rvs when compared with untreated mice and these increases were strengthened by BCAAem, ineffective when supplemented alone (Fig. 8E). Furthermore, given that cells respond to oxidative stress by activating the mitochondrial unfolded protein response (UPR^{mt}), which induces genes that promote ROS detoxification (36), we found a robustly increased

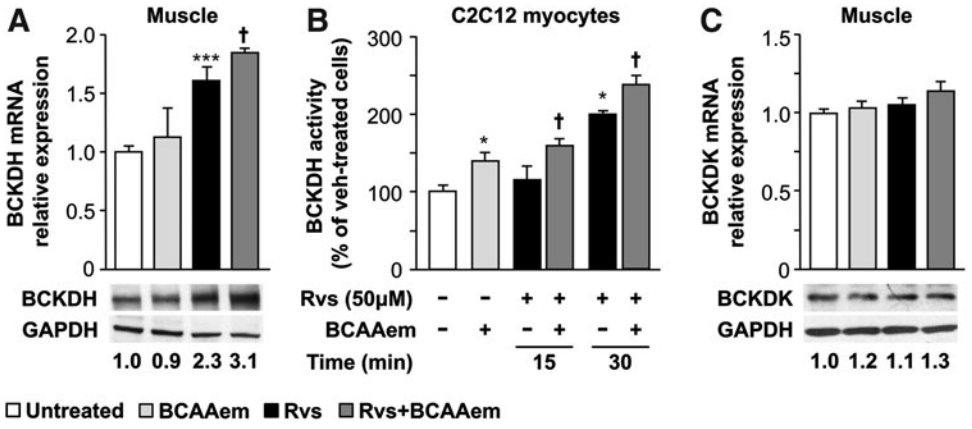

FIG. 6. BCAAem supplementation alone or in combination with Rvs stimulates BCKDH in muscle. (A) and **(C)** BCKDH and BCKDK mRNA (*top*) and protein levels (*bottom*) in vastus lateralis muscle of C57BL/6JN mice treated with Rvs and BCAAem, alone or in combination ($n = 5$ experiments performed in 8–10 animals/group). mRNA levels were analyzed by means of quantitative RT-PCR. GAPDH was served as the standard. Relative expression values of the untreated mice were taken as 1.0. Protein levels were analyzed by means of immunoblot. One experiment representative of three reproducible ones was shown, with relative values of densitometric analysis referred to the vehicle-treated cells taken as 1.0. GAPDH was the loading control. **(B)** BCKDH activity measured in C2C12 myotubes exposed to BCAAem (1×) for 24 h alone or in combination with Rvs (50 μM) added to cell culture for 15 or 30 min ($n = 5$ experiments). $^{*}p < 0.05$, $^{***}p < 0.001$ *versus* vehicle-treated cells; $^{\dagger}p < 0.05$ *versus* Rvs-treated cells. All data are expressed as mean ± SEM. BCKDH, branched-chain α-keto acid dehydrogenase; BCKDK, BCKDH kinase.

expression of CLPP and heat shock protein 60 (HSP60) proteins associated with UPR^{mt} in Rvs and, particularly, in Rvs plus BCAAem relative to untreated C2C12 myocytes (Fig. 8F). Amino acids alone were ineffective to change the UPR^{mt} marker expression. Collectively, these results suggest that Rvs, while impairing mitochondrial function with ROS production, promotes antioxidant defense systems, which are insufficient to prevent muscle toxicity. Notably, BCAAem supplementation exerts a coordinated antioxidant effect, which boosts the antioxidant action of Rvs.

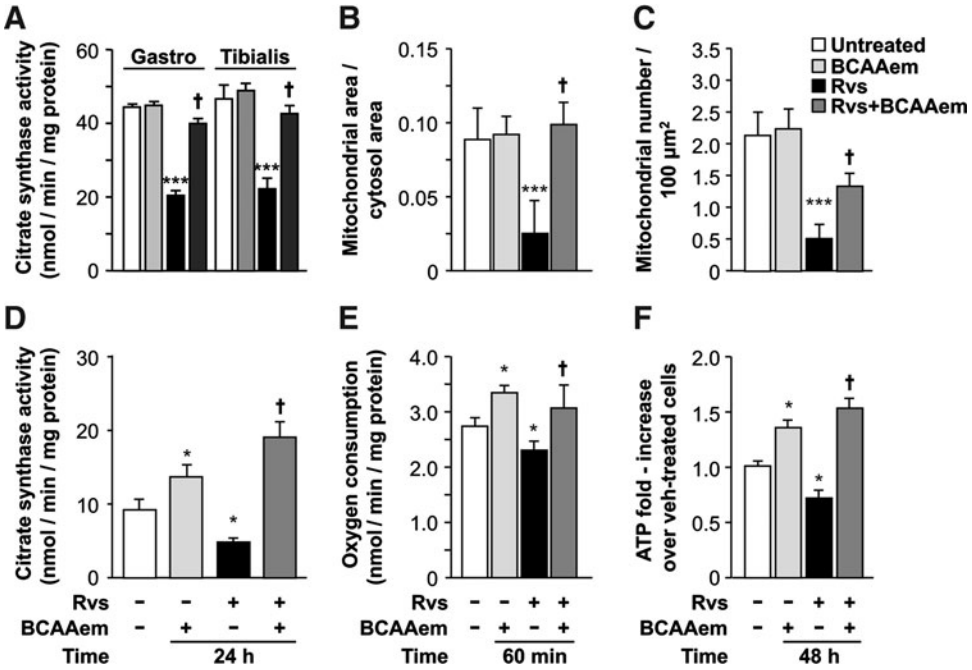

FIG. 7. BCAAem supplementation prevents myopathy induced by Rvs boosting mitochondrial function. (A) CS activity in gastrocnemius and tibialis muscles. **(B)** Mitochondrial area/cytosol area ratio and **(C)** number of mitochondria per 100 μm^2 of cytoplasm, analyzed by electron microscopy in gastrocnemius of mice treated with Rvs and BCAAem ($n = 5$ experiments performed in 8–10 mice/group). All experiments were conducted in C57BL/6JN mice. $^{*}p < 0.05$ and $^{***}p < 0.001$ *versus* corresponding untreated animals; $^{\dagger}p < 0.05$ *versus* corresponding Rvs animals. **(D)** CS activity, **(E)** oxygen consumption, and **(F)** ATP levels in C2C12 myotubes treated with BCAAem (1×) for 24 h with or without Rvs (50 μM). ATP was expressed as fold change *versus* untreated cells taken as 1.0 ($n = 5$ experiments). $^{*}p < 0.05$ *versus* vehicle-treated cells; $^{\dagger}p < 0.05$ *versus* Rvs-treated cells. All data represent mean ± SEM.

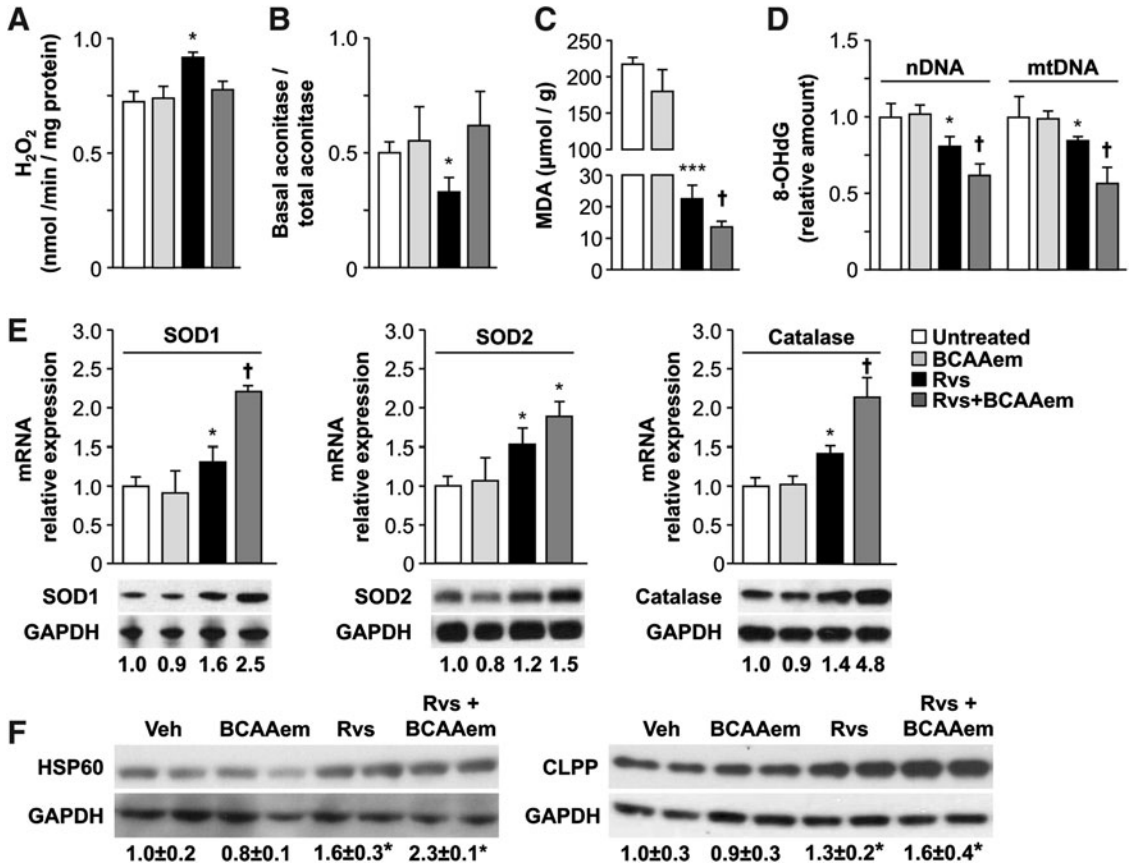

FIG. 8. BCAAem supplementation coordinates an antioxidant effect. **(A)** Mitochondrial H_2O_2 release, **(B)** basal aconitase/total aconitase ratio, **(C)** lipid peroxidation measured as MDA production, and **(D)** nDNA and mtDNA oxidative damage measured as 8-OHdG production in vastus lateralis muscle of Rvs and BCAAem-treated mice ($n = 3$ experiments). **(E)** SOD1, SOD2, and catalase mRNA and protein levels detected by immunoblot in gastrocnemius muscle. mRNA was analyzed by means of quantitative RT-PCR, relative expression values of untreated mice were taken as 1.0 ($n = 3$ experiments), and GAPDH was served as the standard. $^*p < 0.05$, $^{***}p < 0.001$ *versus* untreated mice; $^{\dagger}p < 0.05$ *versus* Rvs-treated mice. All experiments were performed in 8–10 C57BL/6JN mice per group and represent mean ± SEM. **(F)** HSP60 and CLPP proteins detected by immunoblot in C2C12 myotubes treated with Rvs (50 μM) and BCAAem (1×) for 24 h. One experiment representative of five reproducible ones is shown for Western blot images, with values of densitometric analysis referred to GAPDH as a loading control. $^*p < 0.05$ *versus* vehicle-treated cells; $^{\dagger}p < 0.05$ *versus* Rvs-treated mice. Data are expressed as relative values *versus* control taken as 1.0 and reported as mean ± SEM. 8-OHdG, 8-hydroxy-2′-deoxyguanosine; CLPP, caseinolytic peptidase ATP-dependent proteolytic subunit homolog; HSP60, heat shock protein 60; MDA, malondialdehyde; mtDNA, mitochondrial DNA; nDNA, nuclear DNA; SOD, superoxide dismutase.

Discussion

Our data demonstrate that dietary supplementation of BCAAem preserved structure and function of skeletal muscles in mice exposed to chronic treatment with Rvs, without impairing the ability of this drug to lower plasma cholesterol levels. These healthy effects were accompanied both by rescue of *de novo* protein synthesis and reduction of protein breakdown. Moreover, the amino acid formula improved mitochondrial dysfunction of skeletal muscles in the Rvs mice and strengthened the anti-ROS defense mechanisms of statin, with efficacious prevention of oxidative stress in muscle. Although skeletal muscle is a complex tissue comprising a variety of functionally diverse fiber types differently sensitive to statins, we carried out a series of experiments in different muscles (as summarized in Supplementary Table S2) aimed to investigate overall protective mechanisms of BCAAem supplementation without any *a priori* hypothesis. Notably, Westwood *et al.* (69) found a continuum of fiber sensitivity (*i.e.*, necrosis) to high dose of Rvs (150 mg/kg/day), that is, least sensitive, I < IIA < IID < IIB, most sensitive, and that mirrors their oxidative/glycolytic metabolic properties. Rvs did not induce necrosis in the soleus muscle, which contains predominately slow oxidative type I and the more oxidative of the fast fibers, IIC and IIA. Accordingly, we did not observe any functional effects of Rvs and BCAAem on soleus muscle (data not shown).

That BCAAem counteracted reduction of *de novo* protein synthesis and renormalized protein lysis induced by Rvs in C2C12 myotubes is particularly important because the muscle-specific ubiquitin ligase *atrogin-1*/MAFbx has been found recently to mediate lovastatin-induced muscle toxicity in human, zebrafish, and rodent skeletal muscle (30).

A central regulator of proteostasis is mTOR, a serine/threonine protein kinase that regulates many cellular activities besides protein balance, including autophagy, proliferation, survival, and energy metabolism (23). In accord with

several evidences (9, 66), we have observed that Rvs inhibited mTOR activity, measured as Ser2448-mTOR and Thr389-S6K phosphorylation, both in skeletal muscle (gastrocnemius and tibialis) and C2C12 myocytes. Unexpectedly, BCAAem was not able to counteract these effects (data not reported). We cannot rule out that higher doses of amino acids or different time intervals of treatment may be effective both in the *in vivo* and *in vitro* context.

Equally important is that PGC-1α expression was markedly increased in skeletal muscles by BCAAem in combination with Rvs (data not shown). In fact, the overexpression of PGC-1α, a transcriptional coactivator that induces mitochondrial biogenesis and protects against muscle atrophy (49), abrogates lovastatin-mediated *atrogin-1* induction and muscle damage both in mouse myocytes and in zebrafish (30). Moreover, PGC-1α is required for the induction of key ROS-scavenging enzymes (54) and the avoidance of ROS-mediated removal of mitochondria, at least during myogenesis (6). Upregulating endogenous antioxidant levels is a way to increase cell resilience to stress stimuli (in our case, Rvs) beside an index of mitohormesis (*i.e.*, the strategy to augment efficient mitochondria) (47). Again, induction of genes promoting ROS detoxification has been found to follow also UPR^{mt} activation, which promotes mitochondrial homeostasis and cell survival (48). Accordingly, our findings show that BCAAem strengthened the Rvs-induced expression of CLPP, the proteolytic subunit of the ClpXP complex (a major mitochondrial protease), and HSP60 (a mitochondrial chaperone). Both maintain proteostasis and activate UPR^{mt} (36). The hypothesis that efficacy of BCAAem in preventing the Rvs-induced muscle damage may be owed partly to potentiation of the antioxidant effect of statins is in agreement with the results reported by Bouitbir *et al.* (11). Ten days of exercise training of young rats was, indeed, found to increase resistance of plantaris muscle to acute atorvastatin exposure, and this was through combining the effects on mitochondrial function and ROS production. Together, the cellular (proteostasis) and molecular (ROS defense) effects could explain the efficacy of BCAAem to prevent Rvs myopathy.

Moreover, the present work shows that Rvs increased muscle expression and activity of BCKDH, the rate-limiting enzyme of mitochondrial oxidative degradation of BCAAs, and BCAAem strengthened these effects. BCAAs are catabolized mainly in muscle cells (52), where protein turnover is linked to the BCAA catabolic rate (34). Digested BCAAs end up in the bloodstream and are thus readily available for skeletal muscle and other tissues (31). After removal of the amino group by BCATm, carbon skeletons of BCAAs are available for decarboxylation and oxidation to end products that can enter the tricarboxylic acid cycle. The amino group of BCAAs is transferred by BCATm to α-ketoglutarate to form mitochondrial glutamate; thereafter, with different enzymatic reactions, oxaloacetate, glutamine, and alanine formation is increased in the cytoplasm. Interestingly, we reported that both Rvs and BCAAem increased the circulating level of alanine and that these increments are additive (15). Moreover, it is worthy to note that increased BCAA supply and catabolism seem to promote lipid metabolism and fatty acid oxidation associated with a lower risk for metabolic disorders (31). Thus, our findings suggest that Rvs treatment increases protein and amino acid catabolism in skeletal muscles and this can add new insights on the mechanisms of statin myopathy and its prevention. Indeed, a metabolomic analysis has demonstrated that simvastatin changes plasma levels of several amino acids, including threonine, alanine, and phenylalanine, and their degradation products, and these changes have been correlated with LDL cholesterol changes in participants of the Cholesterol and Pharmacogenetics study (58). The authors have suggested that amino acids play an important role in the mechanism of action of simvastatin and can contribute to the inter-individual variation of response to statins.

Clinical relevance of our results is double. First, they suggest that a dietary supplement of amino acids may allow subjects prone to muscle wasting to tolerate statin therapy. Even if with controversial findings, a growing number of rodent and human studies suggest that BCAA-rich protein supplementation has beneficial effects on several health- and fitness-related factors, such as body composition, exercise performance, muscle properties, and glucose control (1, 5, 16). Specifically, BCAAem was found to ameliorate clinical features and complications when administered to patients with disorders of energy metabolism, such as sarcopenia, heart failure, and chronic obstructive pulmonary disease, which are accompanied by muscular damage (2, 3, 18, 19). Second, our data suggest that protection from Rvs myopathy is obtainable, combining simultaneously effects on mitochondrial biology and protein balance. In fact, several approaches have been proposed until now, including coenzyme Q and vitamins to improve mitochondrial defects and quench ROS in myocytes (38) or carnitine to ameliorate protein breakdown (4), yet clinical trials have dismantled these choices (7, 20).

It is important to note that we have studied the effects of only one statin and one amino acid mixture. Other statins and formulas remain to be evaluated. However, deciding which combination of amino acids is most beneficial in this case may be an extremely difficult task. *In silico* strategies have been reported, recently, to study whether amino acid supplementation might be beneficial for increasing muscle contractile protein synthesis (43), yet more than seven amino acid combinations—BCAAem contains 11 amino acids—could not be modeled by the flux model for intrinsic complexity. Finally, further mechanisms modulated by BCAAem and potentially involved in its beneficial effect warrant thorough experimental assessment.

In summary, we unveiled a protective effect of dietary BCAAem on Rvs-induced myopathy. Improved protein metabolism and oxidative stress underlie, at least in part, the protective action of BCAAem. Hence, we propose that nutritional agents able to regulate protein balance and mitochondrial function could be a promising strategy to prevent statin myopathy in humans.

Materials and Methods

Animals and treatments

The experiments were conducted in accordance with European Community Guidelines and Italian Ministry of Health, complied with The National Animal Protection Guidelines, and approved by the Institutional Animal Ethics Committee. C57BL/6JN male mice (8 weeks old, $n=80$) from Charles River were housed in a quiet room with controlled temperature, humidity, and 12-h light/12-h dark cycle and fed with normal chow diet (Laboratorio Dottori Piccioni) (Table 1) (15). Mice were treated with Rvs (20 mg/kg/day, $n=20$) or

BCAAem alone (1.5 mg/g BW/day, $n=20$) or in combination (Rvs + BCAAem, $n=20$) with drinking water for 1 month. BCAAem was dissolved in tap water by calculating average daily drinking 2 weeks before starting treatment. The control group received drinking water without any drug or supplement (untreated; $n=20$). BCAAem composition, relative percentage, and dietary intake of each amino acid are reported in Table 1. The amino acid concentration used was previously found to be active in rodents and mimics the recommended daily dose for humans (16, 45). The dose of Rvs was that normally used in hypercholesterolemic animal models (24, 40). Mice were killed by cervical dislocation, and whole gastrocnemius, soleus, vastus lateralis, and tibialis anterior muscles were rapidly collected and processed for the following analysis (see below). Owing to the limited amount of available material from specific muscles and aimed to investigate overall protective mechanisms of BCAAem supplementation without an *a priori* hypothesis, we carried out a series of experiments in different muscles (as summarized in Supplementary Table S2). On the contrary, only to evaluate any potential effect of BCAAem on the cholesterol-lowering capacity of Rvs, a separate group of 8-week-old Apo-E KO mice ($n=40$), on a mixed 129SvJ and C57BL/6 background (Jackson Labs), were fed on HFD (60% kcal fat) (D12492; Research Diets, Inc.) for 12 weeks and then administered with Rvs and BCAAem following the same schedule described above. Mice had *ad libitum* access to tap water and food.

Plasma analysis

Blood samples were collected between 9:00 and 10:00 a.m. from the retro-orbital sinus. Total cholesterol and TGs were analyzed in ApoE-KO fed mice with HFD using commercially available enzymatic kits (Sentinel Diagnostic). Serum CK level was determined in C57BL/6JN mice using specific kit (Diagnostic Chemicals Limited).

Muscle fiber size and morphometry evaluation

Damage of myocyte nuclei was evaluated by toluidine blue staining in whole gastrocnemius muscle. Morphometric analysis was performed in serial transverse sections (10 μm thick) cut with a Leica CM1850 cryostat and stained with HE. Fiber CSA of gastrocnemius and vastus lateralis muscle was evaluated on 150 fibers/muscle ($n=5$ mice/group) by using an Image 1.63 software (Scion Corporation).

Transmission electron microscopy

Whole gastrocnemius was cut into pieces (1 mm^3) and placed in ice-cold fixative (2.5% glutaraldehyde and 2%

Table 1. Normal Chow Diet and BCAAem Composition and Dietary Intake

			NCD		*BCAAem*[a]		
Nutrient	*Percent*	*Amino acid*	*Percent*[b]	*Dietary intake*[c]	*Percent*[b]	*Dietary intake*[d]	*Δ Dietary intake*
Macronutrient composition							
raw protein	18.8	Arginine	1.15	0.058	—	—	—
		Histidine	0.48	0.024	2.70	0.064	0.040
		Isoleucine	0.80	0.040	15.60	0.274	0.234
		Leucine	1.50	0.075	30.50	0.532	0.457
		Lysine	1.05	0.053	13.20	0.251	0.198
		Methionine+cysteine	0.75	0.038	5.40	0.119	0.081
		Phenylalanine	0.90	0.045	1.60	0.069	0.024
		Threonine	0.75	0.038	10.80	0.200	0.162
		Tryptophan	0.23	0.012	0.20	0.015	0.003
		Valine	1.00	0.050	19.60	0.344	0.294
Crude fat	4.3						
Carbohydrate	76.9						

Micronutrient composition (mg/kg)			
Vitamin A	12,000 UI	Folic acid	2
Vitamin D	1000 UI	Choline chloride	1000
Vitamin E	40	Biotin	0.10
Vitamin B1	8	Iron	100
Vitamin B2	10	Cobalt	0.25
Vitamin B6	10	Copper	3
Pantothenic acid	15	Manganese	55
Vitamin K	1	Iodine	0.80
Vitamin PP	40	Zinc	50
Vitamin B12	0.02	DL-methionine	500

[a]Mice were supplemented with BCAAem in drinking water (1.5 mg/g bw/day, for 1 month).
[b]Amino acid contents are reported as g/100 g food/mouse.
[c]Dietary amino acid intake (g/day) of mice on normal chow diet is determined on average daily food intake.
[d]Dietary amino acid intake (g/day) of mice supplemented with BCAAem is determined on average daily water intake.
BCAAem, branched-chain amino acid-enriched mixture.

paraformaldehyde in 0.1 *M* sodium cacodylate buffer, pH 7.4) for 5 h. Samples were then washed with 0.1 *M* sodium cacodylate buffer, postfixed for 2 h with 2% OsO_4, dehydrated in ethanol, block-stained with uranyl acetate, and embedded in Epon 812 epoxic mixture as reported (15). Ultrathin sections were double stained with uranyl acetate and lead citrate and examined with a Philips CM10 transmission electron microscope. Morphometric analysis of mitochondria was performed as described (67). Randomly selected areas of tissue derived from two animals/group were photographed at a magnification of 5200× and analyzed with NIH Image software.

In vivo *muscle function assessment*

Exercise capacity was assessed in C57BL/6JN mice as previously described (16, 17). Animals were placed on the belt of a 6-lane motorized treadmill (Exer 3/6 Treadmill; Columbus Instruments) supplied with shocker plates (electrical stimulus: 200 ms, 0.34 mA, 1 Hz repetition rate). After acclimatization, mice were subjected to exhaustion treadmill tests at 0° (horizontal treadmill) or to +5° (uphill treadmill) inclination according to the protocol: 5 min at 5 m/min, followed by incremental increase of speed of 1 m/min every minute until exhaustion. Exhaustion was defined as spending time on the shocker plate without attempting to re-engage the treadmill within 20 s. Three tests were performed on each animal, allowing 4 days between each test.

Ex vivo *functional assessment*

Mechanical analysis was performed as described (17). The tibialis anterior muscle of the right leg was dissected, placed in an organ bath filled with Krebs solution (NaCl 120 m*M*, KCl 2.4 m*M*, $CaCl_2$ 2.5 m*M*, $MgSO_4$ 1.2 m*M*, glucose 5.6 m*M*, KH_2PO_4 1.2 m*M*, $NaHCO_3$ 24.8 m*M*, pH 7.4), bubbled with 95% O_2 and 5% CO_2 at 22°C, and attached to a force transducer (Radnoti Organ Bath System; AD Instruments). Electrical pulses were delivered through platinum electrodes connected to a stimulator (Harvard Apparatus). Tetanic isometric contractions were evoked (110 Hz, 500 ms, supramaximal amplitude) at L_o (length at which the maximal isometric force is observed), and the fatigue index was determined from the drop in force of the maximal absolute tetanic force following 20 repeated contractions in a ramp protocol at 0.03, 0.09, and 0.3 Hz. Specific tetanic force is expressed as the normalization of tetanic force over muscle volume. Fatigue index was measured as the tetanic force drop for different stimulation frequencies (from 0.03 to 0.9 Hz, 500 ms) compared with the maximal tetanic force and expressed as percent.

C2C12 cell cultures and treatments

C2C12 myoblasts (<6 passages; ATCC, Manassas, VA) were maintained at 37°C, 5% CO_2, and cultured in Dulbecco's modified Eagle's medium (DMEM) supplemented with 10% fetal bovine serum, 1% penicillin/streptomycin, 1% L-glutamine, and 1% Na^+-pyruvate (EuroClone). Cells were differentiated (C2C12 myocytes) by switching to differentiation medium (DMEM containing 2% horse serum) that was changed daily (27). After 5 days of differentiation, C2C12 myocytes were exposed to Rvs solubilized in sterilized water as appropriate. BCAAem, dissolved in fresh differentiation medium, was added at 1% (1×) for 24 h.

Quantitative real-time polymerase chain reaction

RNA was isolated from muscle or C2C12 myocytes using the RNeasy Mini Kit (Qiagen) and cDNA was synthesized using the iScript cDNA Synthesis Kit (Bio-Rad Laboratories) as described (15). The gene (primer sequences in Table 2) relative level was calculated as $2^{-\Delta\Delta CT}$, in which $\Delta\Delta$CT corresponded to the difference between the ΔCT of either treatment and the ΔCT of the untreated group.

Immunoblot analysis

Protein extracts were obtained from muscle or C2C12 myocytes using T-PER or M-PER Mammalian Protein Extraction Reagent (Pierce; ThermoScientific) as indicated by the manufacturer in the presence of protease and phosphatase inhibitor cocktail (Sigma-Aldrich). Protein content was determined with bicinchoninic acid protein assays (Pierce). An appropriate amount of protein was run on sodium dodecyl sulfate–polyacrylamide gel electrophoresis (SDS-PAGE) under reducing conditions. The proteins were revealed with specific antibodies, anti-Atrogin-1 (Santa Cruz) at 1:250 dilution; anti-BCKDHA (LS Bio), anti-BCKDK, anti-CLPP, and anti-p47phox (from Sigma-Aldrich); anti-SOD1, anti-SOD2, anti-Catalase, and anti-BCATm (from Santa Cruz); anti-Rac1 (Millipore); anti-gp91phox (Becton Dikinson); and anti-HSP60 (Cell Signaling; EuroClone) at 1:1000 dilution. Anti-GAPDH at 1:10,000 dilution (Cell Signaling) was used as loading control. When the Western blot membranes were used for more than one protein, filters were stripped with the Restore Western Blot Stripping Buffer (Pierce) and reincubated with the secondary antibody as suggested by the manufacturer. The amount of protein was measured using SuperSignal Substrate (Pierce) and densitometrically quantified with an IMAGEJ software image analyzer.

De novo *protein synthesis*

C2C12 myocytes were exposed to puromycin (1 μg/ml; Sigma-Aldrich) solubilized in phosphate-buffered saline to measure the *de novo* synthesis of proteins, as described (50). After 10 min of incubation, cells were harvested and proteins were extracted as reported above. Puromycin incorporation was measured by separating 30 μg of denaturated proteins by SDS-PAGE. Total puromycin was revealed with an anti-puromycin antibody (Millipore) at 1:2000 dilution. Anti-vinculin (Sigma-Aldrich) at 1:10,000 dilution was used for normalization.

Branched-chain amino acid catabolism

The BCATm activity was measured spectrophotometrically (340 nm) in cells (14). The samples were homogenized in ice-cold buffer containing 0.4% CHAPSO (Sigma-Aldrich) for the extraction of the enzyme from mitochondrial matrix. After freeze/thawing, cells were centrifuged and the supernatant was used as source of BCATm. The BCKDH activity was evaluated using α-ketoisocaproate (Sigma-Aldrich) as substrate as indicated in Nakai *et al.* (39). Cells were homogenized in ice-cold buffer containing 3% Triton X-100 (Sigma-Aldrich) to extract the enzyme. BCKDH activity was determined spectrophotometrically (355 nm) by measuring the rate of NADH production resulting from the conversion of α-ketoisovalerate to isobutyryl-CoA.

Table 2. Primers Used for PCR Analysis

Gene		*Primer sequences*	*PCR product (bp)*	T_a (°C)
Atrogin-1	Sense	5′-CTTCAACAGACTGGACTTCTCGA-3′	77	60
	Antisense	5′-CAGCTCCAACAGCCTTACTACGT-3′		
BCAT	Sense	5′-AGGTGGGACTGGAGACTGCA-3′	108	60
	Antisense	5′-TTGCCGTACAGCCACAGGAC-3′		
BCKDH	Sense	5′-GCCATCTCCACACCAACCTC-3′	101	60
	Antisense	5′-ACATCGTTGCCGTCCACAC-3′		
BCKDK	Sense	5′-CCCGAATCAACCCCCTCTTC-3′	127	60
	Antisense	5′-TGCAGGGAGCCACCAAGATAC-3′		
SOD1	Sense	5′-GGCTTCTCGTCTTGCTCTC-3′	153	60
	Antisense	5′-AACTGGTTCACCGCTTGC-3′		
SOD2	Sense	5′-GCCTCCCAGACCTGCCTTAC-3′	131	63
	Antisense	5′′-GTGGTACTTCTCCTCGGTGGCG-3′		
Catalase	Sense	5′-CACTGACGAGATGGCACACTTTG-3′	173	63
	Antisense	5′-TGGAGAACCGAACGGCAATAGG-3′		
p47^{phox}	Sense	5′-TGGTGGGTGGTCAGGAAAGG-3′	146	60
	Antisense	5′-CTCTGTGCGTTGCGGATGG-3′		
gp91^{phox}	Sense	5′-GAGTGGTGTGAATGCCAGAGTC-3′	165	60
	Antisense	5′-TGTGATCCCAGCCAACCGAGTC-3′		
Rac1	Sense	5′-ACTAAGTTGCGTTGTGCTGAG-3′	141	60
	Antisense	5′-AAGGAGGCTGTGCTGTGTC-3′		
GAPDH	Sense	5′-AACTTTGGCATTGTGGAAGG-3′	183	60
	Antisense	5′-ACACATTGGGGGTAGGAACA-3′		

GAPDH, glyceraldehyde-3-phosphate dehydrogenase; PCR, polymerase chain reaction; SOD, superoxide dismutase; T_a, temperature of annealing.

Oxygen consumption

Oxygen consumption was measured as described (42, 62). C2C12 myocytes were resuspended in Hank's balanced salt solution. Samples were analyzed at 37°C in a gas-tight vessel equipped with a Clark-type oxygen electrode (Rank Brothers Ltd.) connected to a chart recorder. The oxygen electrode was calibrated assuming the concentration of oxygen in the incubation medium as 200 μmol/l at 37°C.

ATP and CS activity measurements

ATP amount was measured by using specific kit (Molecular Probes; ThermoScientific). ATP was extracted by incubating cells with 1% trichloroacetic acid in 4 mmol/l EDTA solution, 10 min on ice. The extracts were centrifuged (12,000 *g*, 10 min, 4°C) and used for ATP determination as indicated by the manufacturer. CS activity was measured spectrophotometrically (412 nm) at 30°C as previously described (56). Muscle tissue or cells were homogenized and a buffer containing 0.1 mmol/l 5,5-dithio-bis-(2-nitrobenzoic) acid, 0.5 mmol/l oxaloacetate, 50 μmol/l EDTA, 0.31 mmol/l acetyl-CoA, 5 mmol/l triethanolamine hydrochloride, and 0.1 *M* Tris-HCl, pH 8.1 was added. CS activity was expressed as nmol/min/mg of protein.

Mitochondrial oxidative stress

As described in Ref. (16), mitochondria were isolated from muscle using the Qproteome Mitochondria isolation kit (Qiagen). Mitochondrial protein content was determined with BCA assay and 70 μg of mitochondrial proteins was used per sample. Mitochondrial H_2O_2 release was measured in the presence of horseradish peroxidase (HRP), using the Amplex Red Hydrogen Peroxide/Peroxidase Assay kit (Molecular Probes). In the presence of specific substrates, which act as hydrogen donors, the action of HRP converts colorless or nonfluorescent molecules into colored and/or fluorescent moieties, respectively. Amplex Red is a substrate for use with HRP-containing assays. Amplex Red, in the presence of peroxidase enzyme, reacts with H_2O_2 in a 1:1 stoichiometry to produce resorufin, a red fluorescent compound that has an absorption and fluorescence emission maxima of 563 and 587 nm, respectively. Fluorometric measures were made using a Fusion Universal Microplate Analyzer (Packard/PerkinElmer) with excitation filter at 550 nm and emission filter at 590 nm. H_2O_2 production, calculated from a standard curve, was expressed as nmol/min/mg protein (16). Aconitase activity was measured in a medium containing 30 m*M* sodium citrate, 0.6 m*M* $MnCl_2$, 0.2 m*M* NADP, 50 m*M* Tris-HCl, pH 7.4, and 2 U of isocitrate dehydrogenase. The formation of NADPH was followed spectrophotometrically (340 nm) at 25°C as described (33). The level of aconitase activity measured equals active aconitase (basal level). Aconitase inhibited by ROS *in vivo* was reactivated so that total activity could be measured by incubating mitochondrial extracts in a medium containing 50 m*M* dithiothreitol, 0.2 m*M* Na_2S, and 0.2 m*M* ferrous ammonium sulfate. To assay lipid peroxidation in vastus lateralis muscle, malondialdehyde (MDA) derived from polyunsaturated fatty acid peroxides was evaluated by means of the LPO-586 colorimetric assay kit (OxisResearch). Next, to measure the oxidative damage of mitochondrial and nuclear DNA, the highly sensitive 8-OHdG Check ELISA Kit (JalCA) was used in vastus lateralis. Measurements were carried out in accordance with the manufacturer's protocol.

Muscle mitochondria and nuclei were isolated after homogenization of the tissue in an isolation medium comprising 220 m*M* mannitol, 70 m*M* sucrose, 20 m*M* Tris-HCl, 1 m*M* EDTA, 5 m*M* EGTA, and 5 m*M* $MgCl_2$, pH 7.4 (all from Sigma-Aldrich). After centrifugation of samples at 700 *g* 4°C, the nuclear fraction was isolated, whereas the supernatants were collected and transferred into new tubes for subsequent centrifugation at 10,000 *g*, 4°C, to obtained mitochondrial fraction. Mitochondrial and nuclear DNA was extracted using QIamp DNA Mini Kit (Qiagen) and digested with nuclease P1 and alkaline phosphatase (Sigma-Aldrich). The quality and quantity of DNA were confirmed by a NanoDrop ND-1000 spectrophotometry analysis. Absorbance of the ELISA product of reaction was determined spectrophotometrically using 450 nm as the primary wave.

Statistical analyses

All values are expressed as mean ± standard error of the mean. Student's *t*-test was used to evaluate differences between two groups (as indicated). Analyses on four groups were performed using two-way ANOVA, followed by Bonferroni *post-hoc* test for multiple comparisons (GraphPad Prism). Statistical significance was set at p-value <0.05.

Acknowledgments

The authors thank A. Cardile for the first experiments of this project and P. Arcidiaco for analysis of amino acid plasma levels. This work was supported by the Ministero dell'Istruzione, dell'Università e della Ricerca (grants 2009E48P9M_001, 2009 E48P9M_003, and 2010329EKE_002).

Author Disclosure Statement

No competing financial interests exist.

References

1. Adams SH. Emerging perspectives on essential amino acid metabolism in obesity and the insulin-resistant state. *Adv Nutr* 6: 445–456, 2011.
2. Aquilani R, Viglio S, Iadarola P, Opasich C, Testa A, Dioguardi FS, and Pasini E. Oral amino acid supplements improve exercise capacities in elderly patients with chronic heart failure. *Am J Cardiol* 101: 104E–110E, 2008.
3. Aquilani R, D'Antona G, Baiardi P, Gambino A, Iadarola P, Viglio S, Pasini E, Verri M, Barbieri A, and Boschi F. Essential amino acids and exercise tolerance in elderly muscle-depleted subjects with chronic diseases: a rehabilitation without rehabilitation? *Biomed Res Int* 2014: 341603, 2014.
4. Arduini A, Peschechera A, Giannessi F, and Carminati P. Improvement of statin-associated myotoxicity by L-carnitine. *Thromb Haemost* 2: 2270–2271, 2004.
5. Balage M, and Dardevet D. Long-term effects of leucine supplementation on body composition. *Curr Opin Clin Nutr Metab Care* 13: 265–270, 2010.
6. Baldelli S, Aquilano K, and Ciriolo MR. PGC-1alpha buffers ROS-mediated removal of mitochondria during myogenesis. *Cell Death Dis* 5: e1515, 2014.
7. Banach M, Serban C, Ursoniu S, Rysz J, Muntner P, Toth PP, Jones SR, Rizzo M, Glasser SP, Watts GF, Blumenthal RS, Lip GY, Mikhailidis DP, Sahebkar A, and Lipid and Blood Pressure Meta-analysis Collaboration (LBPMC) Group. Statin therapy and plasma coenzyme Q10 concentrations-A systematic review and meta-analysis of placebo-controlled trials. *Pharmacol Res* 99: 329–336, 2015.
8. Bogsrud MP, Langslet G, Ose L, Arnesen KE, Sm Stuen MC, Malt UF, Woldseth B, and Retterstøl K. No effect of combined coenzyme Q10 and selenium supplementation on atorvastatin-induced myopathy. *Scand Cardiovasc J* 47: 80–87, 2013.
9. Bonifacio A, Sanvee GM, Bouitbir J, and Krähenbühl S. The AKT/mTOR signaling pathway plays a key role in statin-induced myotoxicity. *Biochim Biophys Acta* 1853: 1841–1849, 2015.
10. Bouitbir J, Charles AL, Rasseneur L, Dufour S, Piquard F, Geny B, and Zoll J. Atorvastatin treatment reduces exercise capacities in rats: involvement of mitochondrial impairments and oxidative stress. *J Appl Physiol (1985)* 111: 1477–1483, 2011.
11. Bouitbir J, Daussin F, Charles AL, Rasseneur L, Dufour S, Richard R, Piquard F, Geny B, and Zoll J. Mitochondria of trained skeletal muscle are protected from deleterious effects of statins. *Muscle Nerve* 46: 367–373, 2012.
12. Bruckert E, Hayem G, Dejager S, Yau C, and Bégaud B. Mild to moderate muscular symptoms with high-dosage statin therapy in hyperlipidemic patients-the PRIMO study. *Cardiovasc Drugs Ther* 19: 403–414, 2005.
13. Cao P, Hanai J, Tanksale P, Imamura S, Sukhatme VP, and Lecker SH. Statin-induced muscle damage and atrogin-1 induction is the result of a geranylgeranylation defect. *FASEB J* 23: 2844–2854; 2009.
14. Cooper AJ, Conway M, and Hutson SM. A continuous 96-well plate spectrophotometric assay for branched-chain amino acid aminotransferases. *Anal Biochem* 308: 100–105, 2002.
15. Corsetti G, D'Antona G, Ruocco C, Stacchiotti A, Romano C, Tedesco L, Dioguardi F, Rezzani R, and Nisoli E. Dietary supplementation with essential amino acids boosts the beneficial effects of rosuvastatin on mouse kidney. *Amino Acids* 46: 2189–2203, 2014.
16. D'Antona G, Ragni M, Cardile A, Tedesco L, Dossena M, Bruttini F, Caliaro F, Corsetti G, Bottinelli R, Carruba MO, Valerio A, and Nisoli E. Branched-chain amino acid supplementation promotes survival and supports cardiac and skeletal muscle mitochondrial biogenesis in middle-aged mice. *Cell Metab* 12: 362–372, 2010.
17. D'Antona G, Mascaro A, Monopoli A, Miglietta D, Ongini E, and Bottinelli R. Nitric oxide prevents atorvastatin-induced skeletal muscle dysfunction and alterations in mice. *Muscle Nerve* 47: 72–80, 2013.
18. Dal Negro RW, Aquilani R, Bertacco S, Boschi F, Micheletto C, and Tognella S. Comprehensive effects of supplemented essential amino acids in patients with severe COPD and sarcopenia. *Monaldi Arch Chest Dis* 73: 25–33, 2010.
19. Dillon EL, Sheffield-Moore M, Paddon-Jones D, Gilkison C, Sanford AP, Casperson SL, Jiang J, Chinkes DL, and Urban RJ. Amino acid supplementation increases lean body mass, basal muscle protein synthesis, and insulin-like growth factor-I expression in older women. *J Clin Endocrinol Metab* 94: 1630–1637, 2009.
20. DiNicolantonio JJ. CoQ10 and L-carnitine for statin myalgia? *Expert Rev Cardiovasc Ther* 10: 1329–1333, 2012.
21. Dirks AJ, and Jones KM. Statin-induced apoptosis and skeletal myopathy. *Am J Physiol Cell Physiol* 291: C1208–1212, 2006.
22. Draeger A, Monastyrskaya K, Mohaupt M, Hoppeler H, Savolainen H, Allemann C, and Babiychuk EB. Statin

therapy induces ultrastructural damage in skeletal muscle in patients without myalgia. *J Pathol* 210: 94–102, 2006.
23. Efeyan A, Zoncu R, and Sabatini DM. Amino acids and mTORC1: from lysosomes to disease. *Trends Mol Med* 8: 524–533, 2012.
24. Enomoto S, Sata M, Fukuda D, Nakamura K, and Nagai R. Rosuvastatin prevents endothelial cell death and reduces atherosclerotic lesion formation in ApoE-deficient mice. *Biomed Pharmacother* 63: 19–26, 2009.
25. Fang Z, Tang Y, Fang J, Zhou Z, Xing Z, Guo Z, Guo X, Wang W, Jiao W, Xu Z, and Liu Z. Simvastatin inhibits renal cancer cell growth and metastasis via AKT/mTOR, ERK and JAK2/STAT3 pathway. *PLoS One* 8: e62823, 2013.
26. Frantz S, Brandes RP, Hu K, Rammelt K, Wolf J, Scheuermann H, Ertl G, and Bauersachs J. Left ventricular remodeling after myocardial infarction in mice with targeted deletion of the NADPH oxidase subunit gp91PHOX. *Basic Res Cardiol* 101: 127–132, 2006.
27. Fujita H, Nedachi T, and Kanzaki M. Accelerated de novo sarcomere assembly by electric pulse stimulation in C2C12 myotubes. *Exp Cell Res* 313: 1853–1865, 2007.
28. Funabiki R, Watanabe Y, Nishizawa N, and Hareyama S. Quantitative aspect of the myofibrillar protein turnover in transient state on dietary protein depletion and repletion revealed by urinary excretion of N7-methylhistidine. *Biochim Biophys Acta* 451: 143–150, 1976.
29. Gronros J, Wikstrom J, Brandt-Eliasson U, Forsberg GB, Behrendt M, Hansson GI, and Gan LM. Effects of rosuvastatin on cardiovascular morphology and function in an ApoE-knockout mouse model of atherosclerosis. *Am J Physiol Heart Circ Physiol* 295: H2046–2053, 2008.
30. Hanai J, Cao P, Tanksale P, Imamura S, Koshimizu E, Zhao J, Kishi S, Yamashita M, Phillips PS, Sukhatme VP, and Lecker SH. The muscle-specific ubiquitin ligase atrogin-1/MAFbx mediates statin-induced muscle toxicity. *J Clin Invest* 117: 3940–3951, 2007.
31. Kainulainen H, Hulmi JJ, and Kujala UM. Potential role of branched-chain amino acid catabolism in regulating fat oxidation. *Exerc Sport Sci Rev* 4: 194–200, 2013.
32. Liantonio A, Giannuzzi V, Cippone V, Camerino GM, Pierno S, and Camerino DC. Fluvastatin and atorvastatin affect calcium homeostasis of rat skeletal muscle fibers in vivo and in vitro by impairing the sarcoplasmic reticulum/mitochondria Ca2+-release system. *J Pharmacol Exp Ther* 321: 626–634, 2007.
33. Lionetti L, Mollica MP, Crescenzo R, D'Andrea E, Ferraro M, Bianco F, Liverini G, and Iossa S. Skeletal muscle subsarcolemmal mitochondrial dysfunction in high-fat fed rats exhibiting impaired glucose homeostasis. *Int J Obes (Lond)* 31: 1596–1604, 2007.
34. Matthews DE, Motil KJ, Rohrbaugh DK, Burke JF, Young VR, and Bier DM. Measurement of leucine metabolism in man from a primed, continuous infusion of L-[1-3C]leucine. *Am J Physiol* 238: E473–479, 1980.
35. Moßhammer D, Schaeffeler E, Schwab M, and Mörike K. Mechanisms and assessment of statin-related muscular adverse effects. *Br J Clin Pharmacol* 78: 454–466, 2014.
36. Mouchiroud L, Houtkooper RH, Moullan N, Katsyuba E, Ryu D, Cantó C, Mottis A, Jo YS, Viswanathan M, Schoonjans K, Guarente L, and Auwerx J. The NAD(+)/sirtuin pathway modulates longevity through activation of mitochondrial UPR and FOXO signaling. *Cell* 154: 430–441, 2013.
37. Moustardas P, Kadoglou NP, Katsimpoulas M, Kapelouzou A, Kostomitsopoulos N, Karayannacos PE, Kostakis A, and Liapis CD. The complementary effects of atorvastatin and exercise treatment on the composition and stability of the atherosclerotic plaques in ApoE knockout mice. *PLoS One* 9: e108240, 2014.
38. Muraki A, Miyashita K, Mitsuishi M, Tamaki M, Tanaka K, and Itoh H. Coenzyme Q10 reverses mitochondrial dysfunction in atorvastatin-treated mice and increases exercise endurance. *J Appl Physiol (1985)* 113: 479–486, 2012.
39. Nakai N, Kobayashi R, Popov KM, Harris RA, and Shimomura Y. Determination of branched-chain alpha-keto acid dehydrogenase activity state and branched-chain alpha-keto acid dehydrogenase kinase activity and protein in mammalian tissues. *Methods Enzymol* 324: 48–62, 2000.
40. Neto-Ferreira R, Novaes Rocha V, da Silva Torres T, Mandarim-de-Lacerda CA, and de Carvalho JJ. Beneficial effects of rosuvastatin on aortic adverse remodeling in nitric oxide-deficient rats. *Exp Toxicol Pathol* 63: 473–478, 2011.
41. Nicastro H, da Luz CR, Chaves DF, Bechara LR, Voltarelli VA, Rogero MM, and Lancha AH Jr. Does branched-chain amino acids supplementation modulate skeletal muscle remodeling through inflammation modulation? Possible mechanisms of action. *J Nutr Metab* 2012: 136937, 2012.
42. Nisoli E, Clementi E, Paolucci C, Cozzi V, Tonello C, Sciorati C, Bracale R, Valerio A, Francolini M, Moncada S, and Carruba MO. Mitochondrial biogenesis in mammals: the role of endogenous nitric oxide. *Science* 299: 896–899, 2003.
43. Nogiec CD, and Kasif S. To supplement or not to supplement: a metabolic network framework for human nutritional supplements. *PLoS One* 8: e68751, 2013.
44. Omar MA, and Wilson JP. FDA adverse event reports on statin-associated rhabdomyolysis. *Ann Pharmacother* 36: 288–295, 2002.
45. Pellegrino MA, Brocca L, Dioguardi FS, Bottinelli R, and D'Antona G. Effects of voluntary wheel running and amino acid supplementation on skeletal muscle of mice. *Eur J Appl Physiol* 93: 655–664, 2005.
46. Pencina MJ, Navar-Boggan AM, D'Agostino RB, Williams K, Neely B, Sniderman AD, and Peterson ED. Application of new cholesterol guidelines to a population-based sample. *New Engl J Med* 370: 1422–1431, 2014.
47. Ristow M. Unraveling the truth about antioxidants: mitohormesis explains ROS-induced health benefits. *Nat Med* 20: 709–711, 2014.
48. Runkel ED, Baumeister R, and Schulze E. Mitochondrial stress: balancing friend and foe. *Exp Gerontol* 56: 194–201, 2014.
49. Sandri M, Lin J, Handschin C, Yang W, Arany ZP, Lecker SH, Goldberg AL, and Spiegelman BM. PGC-1alpha protects skeletal muscle from atrophy by suppressing $FoxO_3$ action and atrophy-specific gene transcription. *Proc Natl Acad Sci USA* 103: 16260–16265, 2006.
50. Schmidt EK, Clavarino G, Ceppi M, and Pierre P. SUnSET, a nonradioactive method to monitor protein synthesis. *Nat Methods* 6: 275–277, 2009.
51. Schroeter MR, Humboldt T, Schäfer K, and Konstantinides S. Rosuvastatin reduces atherosclerotic lesions and promotes progenitor cell mobilisation and recruitment in apolipoprotein E knockout mice. *Atherosclerosis* 205: 63–73, 2009.
52. Shimomura Y, Murakami T, Nakai N, Nagasaki M, and Harris RA. Exercise promotes BCAA catabolism: effects of BCAA supplementation on skeletal muscle during exercise. *J Nutr* 134: 1583S-1587S, 2004.
53. Sirvent P, Mercier J, Vassort G, and Lacampagne A. Simvastatin triggers mitochondria-induced Ca^{2+} signaling

alteration in skeletal muscle. *Biochem Biophys Res Commun* 329: 1067–1075, 2005.
54. St-Pierre J, Drori S, Uldry M, Silvaggi JM, Rhee J, Jäger S, Handschin C, Zheng K, Lin J, Yang W, Simon DK, Bachoo R, and Spiegelman BM. Suppression of reactive oxygen species and neurodegeneration by the PGC-1 transcriptional coactivators. *Cell* 127: 397–408, 2006.
55. Taylor BA, Lorson L, White CM, and Thompson PD. A randomized trial of coenzyme Q10 in patients with confirmed statin myopathy. *Atherosclerosis* 238: 329–335, 2015.
56. Tedesco L, Valerio A, Dossena M, Cardile A, Ragni M, Pagano C, Pagotto U, Carruba MO, Vettor R, and Nisoli E. Cannabinoid receptor stimulation impairs mitochondrial biogenesis in mouse white adipose tissue, muscle, and liver: the role of eNOS, p38 MAPK, and AMPK pathways. *Diabetes* 59: 2826–2836, 2010.
57. Thompson PD, Clarkson P, and Karas RH. Statin-associated myopathy. *JAMA* 289: 1681–1690, 2003.
58. Trupp M, Zhu H, Wikoff WR, Baillie RA, Zeng ZB, Karp PD, Fiehn O, Krauss RM, and Kaddurah-Daouk R. Metabolomics reveals amino acids contribute to variation in response to simvastatin treatment. *PLoS One* 7: e38386, 2012.
59. Tuckow AP, Jefferson SJ, Kimball SR, and Jefferson LS. Simvastatin represses protein synthesis in the muscle-derived C2C12 cell line with a concomitant reduction in eukaryotic initiation factor 2B expression. *Am J Physiol Endocrinol Metab* 300: E564–570, 2011.
60. Ucar M, Mjörndal T, and Dahlqvist R. HMG-CoA reductase inhibitors and myotoxicity. *Drug Saf* 22: 441–457, 2000.
61. Valencak TG, and Azzu V. Making heads or tails of mitochondrial membranes in longevity and aging: a role for comparative studies. *Longev Healthspan* 3: 3, 2014.
62. Valerio A, Cardile A, Cozzi V, Bracale R, Tedesco L, Pisconti A, Palomba L, Cantoni O, Clementi E, Moncada S, Carruba MO, and Nisoli E. TNF-α downregulates eNOS expression and mitochondrial biogenesis in fat and muscle of obese rodents. *J Clin Invest* 116: 2791–2798, 2006.
63. Valerio A, D'Antona G, and Nisoli E. Branched-chain amino acids, mitochondrial biogenesis, and healthspan: an evolutionary perspective. *Aging (Albany NY)* 3: 464–478, 2011.
64. van Staa TP, Carr DF, O'Meara H, McCann G, and Pirmohamed M. Predictors and outcomes of increases in creatine phosphokinase concentrations or rhabdomyolysis risk during statin treatment. *Br J Clin Pharmacol* 78: 649–659, 2014.
65. Wagner BK, Kitami T, Gilbert TJ, Peck D, Ramanathan A, Schreiber SL, Golub TR, and Mootha VK. Large-scale chemical dissection of mitochondrial function. *Nat Biotechnol* 26: 343–351, 2008.
66. Wei YM, Li X, Xu M, Abais JM, Chen Y, Riebling CR, Boini KM, Li PL, and Zhang Y. Enhancement of autophagy by simvastatin through inhibition of Rac1-mTOR signaling pathway in coronary arterial myocytes. *Cell Physiol Biochem* 31: 925–937, 2013.
67. Weibel ER. Practical methods for biological morphometry. In: *Stereological Methods*, Volume 1. London, UK: Academic Press, 1979, pp. 40–116.
68. Westwood FR, Bigley A, Randall K, Marsden AM, and Scott RC. Statin-induced muscle necrosis in the rat: distribution, development, and fibre selectivity. *Toxicol Pathol* 33: 246–257, 2005.
69. Westwood FR, Scott RC, Marsden AM, Bigley A, and Randall K. Rosuvastatin: characterization of induced myopathy in the rat. *Toxicol Pathol* 36: 345–352, 2008.
70. Woodard J, Sassano A, Hay N, and Platanias LC. Statin-dependent suppression of the Akt/mammalian target of rapamycin signaling cascade and programmed cell death 4 up-regulation in renal cell carcinoma. *Clin Cancer Res* 14: 4640–4649, 2008.

Address correspondence to:
Prof. Enzo Nisoli
Department of Medical Biotechnology and Translational Medicine
Center for Study and Research on Obesity
Milan University
via Vanvitelli, 32
20129 Milan
Italy

E-mail: enzo.nisoli@unimi.it

Date of first submission to ARS Central, November 22, 2015; date of final revised submission, May 16, 2016; date of acceptance, May 23, 2016.

Abbreviations Used

3-MeH = 3-methylhistidine
8-OHdG = 8-hydroxy-2′-deoxyguanosine
ApoE-KO = apolipoprotein E gene-deficient
BCAA = branched-chain amino acid
BCAAem = branched-chain amino acid-enriched mixture
BCATm = mitochondrial branched-chain aminotransferase
BCKDH = branched-chain α-keto acid dehydrogenase
BCKDK = branched-chain α-keto acid dehydrogenase kinase
BW = body weight
CK = creatine kinase
CLPP = caseinolytic peptidase ATP-dependent proteolytic subunit homolog
CS = citrate synthase
CSA = cross-sectional area
DMEM = Dulbecco's modified Eagle's medium
GAPDH = glyceraldehyde-3-phosphate dehydrogenase
HE = hematoxylin–eosin
HFD = high-fat diet
HSP60 = heat shock protein 60
MAFbx = muscle atrophy F-Box
MDA = malondialdehyde
mTOR = mechanistic/mammalian target of rapamycin
MW = muscle weight
PGC-1α = peroxisome proliferator-activated receptor gamma coactivator-1 α
phox = phagocyte oxidase
Rac1 = Ras-related C3 botulinum toxin substrate 1
Rvs = rosuvastatin
ROS = reactive oxygen species
SDS-PAGE = sodium dodecyl sulfate–polyacrylamide gel electrophoresis
SOD = superoxide dismutase
T-Cho = total cholesterol
TG = triglyceride
UPR^{mt} = mitochondrial unfolded protein response